

Berberine Protects Glomerular Podocytes via Inhibiting Drp1-Mediated Mitochondrial Fission and Dysfunction

Xin Qin¹, Yan Zhao², Jing Gong², Wenya Huang², Hao Su¹, Fen Yuan¹, Ke Fang², Dingkun Wang², Jingbin Li², Xin Zou¹, Lijun Xu¹, Hui Dong¹✉, Fuer Lu¹✉

1. Institute of Integrated Traditional Chinese and Western Medicine, Tongji Hospital, Tongji Medical College, Huazhong University of Science and Technology, Wuhan, China
2. Department of Integrated Traditional Chinese and Western Medicine, Tongji Hospital, Tongji Medical College, Huazhong University of Science and Technology, Wuhan, China

✉ Corresponding authors: Hui Dong, e-mail: tjhdonghui@163.com; Fuer Lu, e-mail: felu@tjh.tjmu.edu.cn

© Ivyspring International Publisher. This is an open access article distributed under the terms of the Creative Commons Attribution (CC BY-NC) license (<https://creativecommons.org/licenses/by-nc/4.0/>). See <http://ivyspring.com/terms> for full terms and conditions.

Received: 2018.10.12; Accepted: 2019.01.13; Published: 2019.02.28

Abstract

Elevated levels of plasma free fatty acid (FFA) and disturbed mitochondrial dynamics play crucial roles in the pathogenesis of diabetic kidney disease (DKD). However, the mechanisms by which FFA leads to mitochondrial damage in glomerular podocytes of DKD and the effects of Berberine (BBR) on podocytes are not fully understood.

Methods: Using the db/db diabetic mice model and cultured mouse podocytes, we investigated the molecular mechanism of FFA-induced disturbance of mitochondrial dynamics in podocytes and testified the effects of BBR on regulating mitochondrial dysfunction, podocyte apoptosis and glomerulopathy in the progression of DKD.

Results: Intragastric administration of BBR for 8 weeks in db/db mice significantly reversed glucose and lipid metabolism disorders, podocyte damage, basement membrane thickening, mesangial expansion and glomerulosclerosis. BBR strongly inhibited podocyte apoptosis, increased reactive oxygen species (ROS) generation, mitochondrial fragmentation and dysfunction both *in vivo* and *in vitro*. Mechanistically, BBR could stabilize mitochondrial morphology in podocytes via abolishing palmitic acid (PA)-induced activation of dynamin-related protein 1 (Drp1).

Conclusions: Our study demonstrated for the first time that BBR may have a previously unrecognized role in protecting glomerulus and podocytes via positively regulating Drp1-mediated mitochondrial dynamics. It might serve as a novel therapeutic drug for the treatment of DKD.

Key words: diabetic kidney disease, podocyte, mitochondrial fission, dynamin-related protein 1, Berberine

Introduction

Mitochondria are dynamic organelles that consistently undergo fusion and fission, frequently changing their number and shape to adapt to variations in metabolic demands. Mitochondrial fission regulates mitochondrial biogenesis and mitophagy, whereas mitochondrial fusion controls proper distribution of mitochondrial DNA (mtDNA) and metabolic substance across all mitochondria[1, 2]. Under physiological conditions, the harmonization of mitochondrial dynamics guarantee efficient oxidative phosphorylation (OXPHOS) and adenosine

triphosphate (ATP) production in cells with elongated and filamentous mitochondria[3]. However, the mitochondrial dynamic balance will shift to fission when cells are under metabolic or environmental stresses. This is accompanied by a fragmented morphology, compromised energy metabolism, increased content of reactive oxygen species (ROS) and loss of mitochondrial membrane potential (MMP). Excessive mitochondrial ROS can in return lead to mitochondrial disruption including mtDNA damage and mutations and the release of pro-apoptotic

proteins[4].

Mitochondrial fission is typically regulated by dynamin-related protein 1 (Drp1), a dynamin family member that binds to its receptors on mitochondrial outer membrane (MOM) and assembles a larger oligomer, which finally splits mitochondrial tubules into fragments[2, 5]. Mediators that promote Drp1 translocating to the MOM, increase Drp1 expression, or regulate the post-translational modification of Drp1 all contribute to mitochondrial fission[6, 7]. Drp1 may interact with Bax to promote the permeability of MOM, resulting in the release of mitochondrial apoptotic proteins (for example, cytochrome c) to the cytoplasm. These proapoptotic proteins then activate signaling cascade of caspases, eventually resulting in cell apoptosis[8]. Drp1 knockdown or pharmacologic inhibition by Mdivi1 could be sufficient to block these signaling cascades, thereby preventing mitochondrial fission-induced cell apoptosis[9].

Recent advances focusing on mitochondrial biology have proposed that excessive mitochondrial fission and mitochondrial dysfunction in podocytes are typical features of kidney injury, but preceding the clinical manifestations of diabetic kidney disease (DKD) [10]. Podocytes are terminally differentiated epithelial cells that form interdigitated foot processes (FPs) constituting the crucial component of the glomerular filtration barrier (GFB) to protein leakage [11]. Podocyte injury, dedifferentiation and loss are pathological hallmarks of DKD, preceding albuminuria and then exacerbating proteinuria and glomerular sclerosis[12]. Given that kidney cells need continuous high levels of energy consumption and the mitochondrial OXPHOS is the primary source of ATP production, there exist abundant mitochondria in glomerular cells[13]. However, persistent hyperglycemia and dyslipidemia in DKD condition can induce podocyte mitochondrial dysfunction as well as excessive mitochondrial fission followed by a range of alterations, including elevated ROS production, cell apoptosis and detachment, which ultimately induce GFB destruction and proteinuria[14, 15]. Remarkably, increased mitochondrial ROS (mtROS) in podocytes is considered as the critical links for certain pivotal pathogenic mechanisms involving in the glomerulusclerosis and progression of DKD[16, 17].

Deregulated lipid metabolism with abnormal FFA metabolism is the typical complication of T2DM [18]. Palmitic acid (PA) is the most abundant FFA in humans and rodents plasma that accounts for 25 percent of total content[19]. The total plasma FFA level can increase up to fourfold in T2DM[20]. Increased FFA content could cause damage to target organs in DM patients, inducing ROS overproduction, mitochondrial dysfunction and MOM permeability-

mediated cytochrome c release followed by cell apoptosis[21]. Glomerular podocytes are highly sensitive to FFA. Enhanced FFA uptake by podocytes could lead to intracellular lipid accumulation and peroxidation[22]. The excess cellular ROS in response to high concentrations of FFA is the main culprit for podocyte injury in DKD[23].

Berberine (BBR) is a kind of isoquinoline alkaloid present in Chinese herbal medicines and widely used for treating diarrhea and diabetes mellitus (DM)[24]. BBR has been demonstrated to have various of metabolic benefits, including hypoglycemic and hypolipidemic roles[25], improvement of insulin resistance[26] and oxidative damage[27]. Combining the therapeutic effects of BBR with recent observations suggesting Drp1-mediated mitochondrial dynamics as new potential targets against DKD, we hypothesized that BBR might prevent the progression of DKD through regulating Drp1 in podocytes. Our findings clearly showed that podocytes are highly susceptible to PA, which induced cell damage and apoptosis via disturbing mitochondrial morphology and function. Further we demonstrated that BBR significantly attenuated excessive mitochondrial fission, mitochondrial dysfunction and ROS overproduction, which protected podocytes from apoptosis and detachment, thus dramatically preventing the pathological progress of DKD.

Methods

Cell culture

Conditionally immortalized mouse podocyte established and distributed by Professor Peter Mundel of the Medical College of Harvard University (Boston, MA, USA) was provided by First Affiliated Hospital of Peking University (Beijing, China). Cultivation of podocytes was performed as previously reported [28]. To induce differentiation (non-permissive condition), podocytes were cultivated without IFN- γ at 37 °C for 10 days. For subsequent experiments, differentiated podocytes were pretreated with 0.4 μ mol/L BBR (Sigma-Aldrich, MO, USA) or 10 μ mol/L Mdivi1 (MCE, NJ, USA) or basic medium for 12 h. The next day, cells were cultured in medium containing 100 μ mol/L PA for 12 h.

Palmitate

First, palmitate (Sigma-Aldrich, MO, USA) was dissolved in sodium hydroxide solution (0.1 M) at 70 °C for 30 min to form sodium palmitate (40 mM). Palmitate was then combined with fatty-acid-free BSA (Solarbio, Beijing, China). BSA (40%) was dissolved in PBS and added dropwise into the palmitate solution. Then the mixed solution was maintained at 55°C for 30 min. Finally, the PA stock (20 mmol/L) was filtered

and stored at -20 °C until use.

Cell apoptosis assay

For annexin V/PI labeling, cells were incubated with annexin V followed by PI staining (BD Biosciences, USA) according to the manufacturer's instruction. After adding 400 μ l 1X Binding Buffer, samples were analyzed immediately by flow cytometry (BD FACSCalibur, USA).

Assessment of ROS generation

ROS content was measured with the ROS-sensitive fluorescent probe, 2',7'-dichlorodihydrofluorescein diacetate (DCFH-DA). After the treatment, podocytes were incubated with 20 μ M DCFH-DA at 37°C in the dark for 30 min. Green fluorescence derived from cellular ROS generation was detected by flow cytometry with 525 nm for emission (FACS Aria) or observed by the fluorescence microscope (Nikon, Tokyo, Japan). More than 10,000 cells were acquired for each sample, and the ROS level was quantified by mean fluorescence intensity.

The lipid peroxidation products malondialdehyde (MDA) in podocytes was measured according to procedures of manufacturer (Jiancheng, Nanjing, China) as reported previously[29].

To assess production of superoxide in kidney glomerular, dihydroethidium (DHE), the O₂-sensitive fluorescent dye, was used as previously described [30]. Unfixed frozen kidney sections were incubated with 1 μ mol/L DHE at 37°C in dark for 30 minutes and then coverslipped. Tissue sections were then observed with a fluorescence microscope.

Measurement of ATP levels

Contents of ATP were assessed with a bioluminescence assay kit (Beyotime, Shanghai, China). The measurement was conducted as previously described [31]. After the treatment, supernatants were removed and podocytes were lysed in the ATP assay buffer for 5 min. Cells from each well were then collected for centrifugation. The supernatant fraction was put into a 96-well clear bottom, black-walled microplate (Corning Incorporated, NY, USA) and then luciferase reagent was added. The luminescence was detected by a luminometer (Synergy, BioTek Instruments, USA).

MMP measurement

MMP was determined using the lipophilic cationic dye JC-1 (Beyotime, Shanghai, China) as described previously[31]. The ratio of red to green (590/520) fluorescence reflects the MMP. In this experiment, podocytes were loaded with JC-1 in the dark for 20 min and fluorescence was measured by flow cytometry. For imaging, cells were observed by

the fluorescence microscope.

Transmission electron microscopy (TEM)

To analyze ultrastructure changes in the glomerulus and podocyte mitochondria, Kidney tissues and podocytes were fixed in 2% glutaraldehyde for 12 h at 4°C, then post-fixed in 1% osmium tetroxide. Fixed sections were dehydrated in ascending concentrations of ethanol, then infiltrated, embedded and sliced with ultramicrotome. Uranyl acetate and lead citrate were used to stain the sections. Finally, the transmission electron microscope (Hitachi, Tokyo, Japan) was used for examining and photographing these sections.

Extraction of podocytes and glomerular mitochondria

Mitochondria from podocytes were isolated using a mitochondria isolation kit (Thermo Fisher Scientific, USA) according to the manufacturer's protocol. Isolated mitochondria were lysed in buffer and the protein concentration were measured by the Bradford method.

Western blot analyses

Western blotting was performed according to the standard methods. Briefly, samples were lysed in buffer on ice and then centrifuged. Protein concentrations were measured with a BCA Protein Assay Kit. The lysates were mixed with loading buffer and boiled for 10 min. Protein samples (60 μ g each group) were loaded on SDS-PAGE, separated and transferred to polyvinylidene fluoride membrane using standard procedures. Membranes were then probed with appropriate antibodies. The detection of signal was pictured with the Odyssey Infrared Imaging System (LI-COR Biosciences, Lincoln, NE). Anti-COX IV and β -actin antibody were used as loading controls for mitochondria and cytoplasm respectively. The antibodies used in this study are listed in Supplementary Table S1.

Immunofluorescence and Immunohistochemistry

For mitochondria staining in cultured podocytes, cells were grown on glass coverslips and mitochondrial morphology was visualized by labeling the cells with 50 nmol/L MitoTracker Red CMXRos (Thermo Fisher Scientific, USA) in the dark for 30 min at 37°C. Images were then acquired by laser scanning confocal microscopy (Leica Microsystems, 100X oil objective).

For mitochondria colocalization with Drp1, podocytes were pretreated with 50 nM MitoTracker Red first. They were then fixed paraformaldehyde, blocked with certain serum and incubated with

appropriate primary antibodies and FITC-labeled secondary antibody. Nuclei was counterstained with DAPI for 5 min. Staining was observed by a fluorescence microscope or the confocal microscopy.

For kidney paraffin sections, after dewaxing, rehydration, antigen retrieval, reducing endogenous peroxidase activity and blocking, sections were then incubated with primary antibodies and HRP or FITC-conjugated anti-rabbit/anti-mouse secondary antibodies and then observed with fluorescence microscope. Glomerular podocytes in kidney tissues were specially labeled with podocin.

Analyses of mitochondrial morphology

Mitochondrial shape and size were measured and quantified using Image J (National Institutes of Health, Bethesda, MD) as previously described [32-34]. For immunofluorescence images, computer-assisted quantitative analyses were used for tracing the mitochondrial branches. Punctate was defined as cells with spherical shape (no clear length or width). Rod indicated individual mitochondria with a tubular structure, and network was defined as cells with highly interconnected mitochondria.

For TEM micrographs, we manually traced only clearly discernible outlines of mitochondria. Morphological parameters including surface area, perimeter, the longitudinal length (major axis) and equatorial length (minor axis) were measured automatically by the Image J software. The aspect ratio [AR, (major axis)/(minor axis)] and form factor [FF, (perimeter²)/(4π surface area)] which reflect the branching aspect of mitochondria were calculated. Both AR and FF have a minimal value of 1 that indicates a small perfect spheroid. Increase of the values represents the shape becoming elongated and branched. Circularity [4π (surface area/perimeter²)] and roundness [4 (surface area)/(π major axis²)] were calculated as indexes of sphericity with a maximum value of 1 indicating a perfect circle.

Quantitative real-time PCR

RNA was extracted from samples using the Trizol reagent (Takara, Japan). The Thermo Scientific NanoDrop spectrophotometer was used to detect the purity and concentration of RNA. Then, cDNA was synthesized using the reverse transcriptase kit (Takara, Japan). Quantitative analysis of mRNA expression was conducted with a SYBR premix EX TaqTM kit (Takara, Japan) with StepOne PCR system (Applied Biosystems, USA). The relative quantity of mRNA was expressed as $2^{-\Delta\Delta CT}$. Sequences of the primers are listed in Supplementary Table S2.

mtDNA content quantification

To evaluate mtDNA copy number, NADH

dehydrogenase subunit 1 (ND1) encoded on the mitochondrial genome were used as mtDNA marker. 18S ribosomal RNA served as an endogenous control. Quantitative Real-Time PCR was conducted according to the standard methods described previously [35].

Lentiviral infection

For preparation of Drp1 overexpression podocytes, mouse Drp1 overexpressing lentiviral particles were used with the scramble lentiviral particles (Gene, Shanghai, China) as control. Cells were first seeded in plates. Then they were infected with lentivirus stock and 8 μg/ml Polybrene (Santa Cruz Biotechnology, Santa Cruz, USA) and incubated for 12 h. Cells were then switched to normal culture medium and selected with 2 μg/ml puromycin (TOCRIS). The expression of Drp1 was examined by western blotting and quantitative-RT PCR. After lentiviral transfection, the cells were treated with BBR or PA for subsequent experiments.

siRNA-mediated gene silencing

Podocytes were grown to 40% confluent in six-well plates. Drp1 siRNA and control siRNA (Ruibio, Guangzhou, China) were transfected into cells using GenMute transfection reagent (SigmaGen, USA) at 50 nmol/L of siRNA according to manufacturer's protocol. More than 90% of cells were successfully infected as indicated by GFP expression after 36 h. After siRNA transfection, the cells were treated with BBR or PA for subsequent experiments.

Animal experiments

Animal maintenance and all experimental procedures were conducted according to the NIH guidelines for use of laboratory animals with approval of the Animal Care Committee of Huazhong University of Science and technology (Wuhan, China). Male db/db diabetic mice and the nondiabetic littermates (7 weeks old) were purchased from the Model Animal Research Center of Nanjing University and socially housed at a constant temperature of 22°C ± 2°C with a 12:12 h light/dark cycle. Diabetic db/db mice were randomly separated into different groups (db/db and db/db + BBR; n = 10 in each subgroup) and treated with either BBR (300 mg/kg/d) or vehicle by gavage for the next 8 weeks. BBR dosage used in our experiment was chosen according to animal studies and clinical trials previously reported[36-38]. Fasting blood glucose (FBG) and body weight were monitored at 11 and 15 weeks of age. After intervention, urinary albumin and creatinine concentration were also measured by the ELISA kit. Then all experimental subjects were killed under anesthesia. The distal parts of each kidney were either

fixed overnight with 4% formaldehyde or preserved at -80°C. Mouse glomeruli and podocytes were isolated according to the methods previously reported before conducting western blotting and PCR[9, 39]. For outcome assessments, a minimum of five mice per group were examined by investigators.

Kidney Histopathology

After mouse was anesthetized, kidneys were taken out immediately and cut in half. The distal parts of each kidney were fixed overnight with 4% formaldehyde, embedded in paraffin, and then sliced at a thickness of 5 µm. For morphometric lesion analysis, hematoxylin-eosin (HE) and periodic acid-schiff (PAS) were conducted. The general histologic changes in mouse glomeruli including glomerular volume, the mesangial area and glomerular basement membrane were determined. Five mice per group and a minimum of 50 glomeruli in three sections per animal were examined.

Tissue FFA analyses

FFA content in kidney podocytes were measured using the FFA quantification kit (Abcam) following the manufacturer's instruction. Briefly, the samples were homogenized in buffer and protein concentration was measured by Bradford assay. The homogenate was mixed with chloroform and centrifuged. Then the organic phase was collected and the lipids in which were dried and dissolved in Free Acid Assay Buffer for measurement. The FFA content were normalized to protein concentration.

Statistical Analyses

All the data were expressed as mean ± SEM, except morphological parameters of mitochondria shown as the median (interquartile range). Multiple groups were compared by performing one-way ANOVA following Tukey multiple comparisons tests. *P*-values < 0.05 were considered as statistically significant and all tests were two tailed. GraphPad Prism software (GraphPad Software, La Jolla, CA) was used for performing the tests.

Results

Effects of BBR on PA-induced podocyte damage and apoptosis

The protective effects of BBR on podocytes were tested using cultured mouse podocyte (MPC-5). We first examined those important slit diaphragm proteins (SDs) forming between adjacent interdigitating podocyte FPs[12]. As shown in Figure 1A-B, the protein expressions of nephrin, podocin and CD2AP in podocytes cultured with PA markedly decreased. However, the SDs levels increased with the treatment

of BBR as well as Mdivi1. Besides, BBR and Mdivi1 greatly repressed the protein expressions of desmin and matrix metalloproteinase-9 (MMP-9) which are the markers of podocyte injury and dedifferentiation [40, 41].

We next detected the role of BBR on PA-induced cell apoptosis and caspase 3 activation. As shown in Figure 1C, BBR treatment strongly suppressed podocyte apoptosis assessed by annexin V/PI staining. Through the TEM we observed PA-induced condensation of chromatin which is the essential step and hallmark of morphologic changes in the nucleus during apoptosis[42]. The abnormal changes were restored with the treatment of BBR (Figure 1D). The results also showed that BBR could promote autophagy in cells under stress conditions, in accordance with previous findings[43]. Besides, BBR lowered the level of activated caspase 3 and elevated the expression of antiapoptotic protein Bcl2 (Figure 1E).

Previous studies have shown that under stress conditions, Bax can be activated and translocate from the cytosol to the mitochondria, promoting the release of cytochrome c and cell apoptosis[8]. Accordingly, we found that mitochondria Bax (mtBax) and cytosolic cytochrome c increased in cells upon their exposure to PA (Figure 1F). However, both were strongly abolished by BBR treatment. These data indicated that BBR could protect podocytes from PA-induced damage and apoptosis.

BBR inhibits PA-induced mtROS production, mitochondrial dysfunction and fragmentation in podocytes

As byproduct of electron transport, ROS generated in the mitochondria can take up about 80% of superoxide produced in the basal state. Under stress conditions, mtROS production induces mtDNA damage and mutations followed by cell apoptosis. Thus, ROS is both the marker and chief culprit of mitochondrial dysfunction and damage[4]. As shown in Figure 2A-B, PA-induced intracellular ROS generation, measured by staining DCFH-DA fluorescence dye using fluorescence microscope and flow cytometry, was significantly increased. It was similar to that of pro-oxidants H₂O₂ (1 µmol/L). BBR, Mdivi1, as well as total antioxidant N-acetylcysteine (NAC)[44] and mitochondrial antioxidant mito-tempol[45], blocked ROS production in podocytes, except for cytosol antioxidant nordihydroguaiaretic acid (NDGA)[46].

Mitochondrial oxidative stress can disturb the MMP and ATP synthesis which reflect mitochondrial function[47]. In the present study, we observed PA-induced disruption of MMP and ATP production,

and both were reversed with the treatment of BBR or Mdivi1(Figure 2C-E). BBR also reduced lipid peroxidation products-MDA, as shown in Figure 2F.

We next examined alterations of mitochondrial ultrastructure by using TEM. As shown in Figure 3A, cells treated with PA showed small punctate and rounded mitochondria when compared with controls. However, mitochondria from BBR-treated cells phenocopied those from Mdivi1 treatment, displaying interconnected, filamentous and tubular shape. For quantitative analysis of mitochondrial morphology, a series of parameters were used, including aspect ratio

and form factor with bigger values indicating more elongated mitochondria (Figure 3A-B) and circularity and roundness with bigger values indicating more rounded mitochondria (Figure 3B). Besides, mitochondrial length was measured, as shown in Figure 3C. Mitochondrial morphology visualized by mitochondrial fluorescent probe (MitoTracker Red CMXRos) also showed the similar change (Figure 3D-E). Collectively, these results suggested that the protective roles of BBR in podocytes were possibly through eliminating mitochondrial ROS and modulating mitochondria morphology and function.

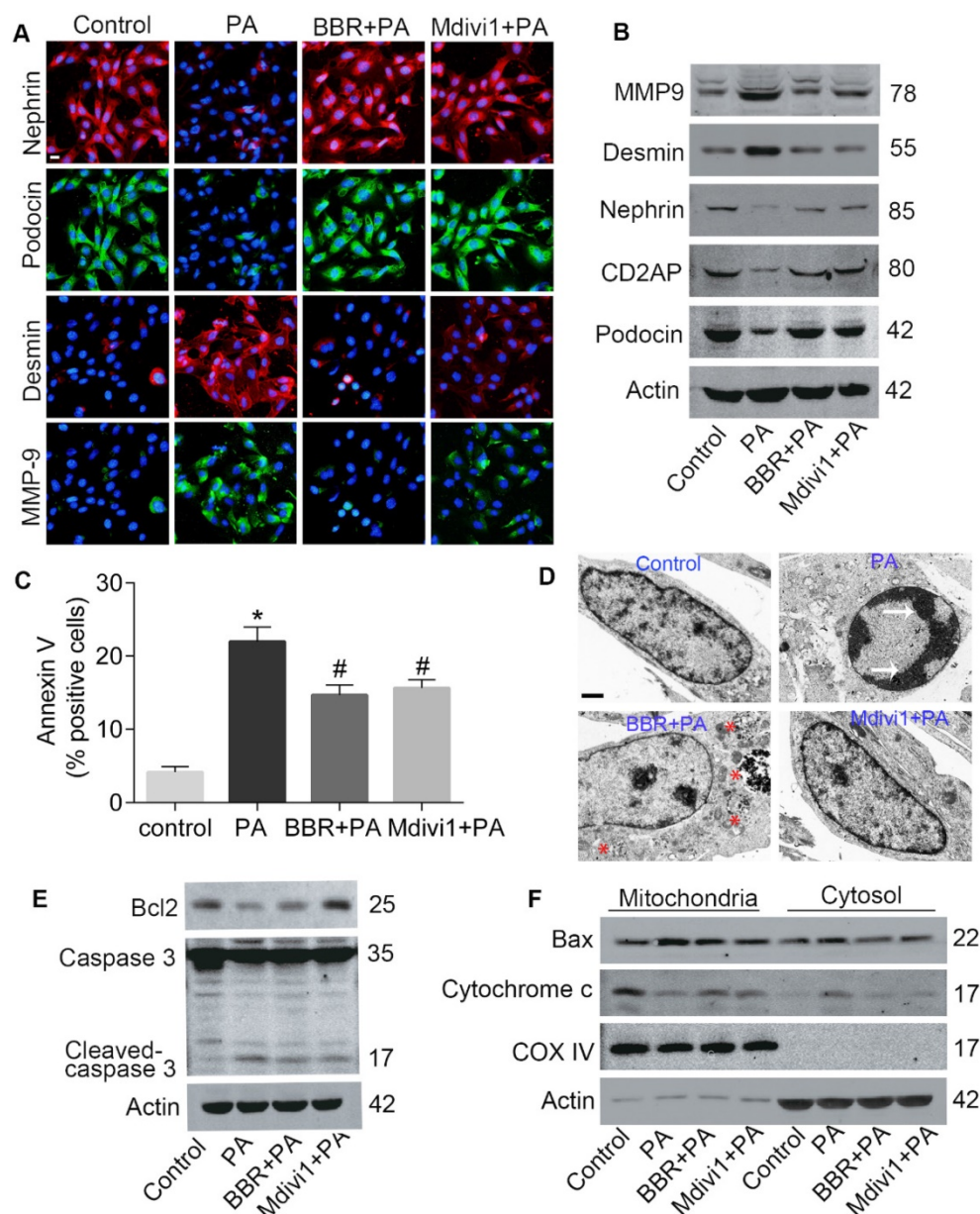


Figure 1. Effects of BBR on PA-induced podocyte injury and apoptosis. (A) SDs and markers of podocyte dedifferentiation were analyzed by fluorescence microscopy. Nephrin, red; Podocin, green; Desmin, red; MMP-9, green. Scale bars, 50 μ m. (B) Western blotting of SDs and markers of podocyte dedifferentiation. (C) Cell apoptosis was assessed by flow cytometry after annexin V/PI staining. Annexin V positive cells indicate early apoptosis. (D) Cell apoptosis related condensation of chromatin in nucleus and autophagy were observed using TEM. Arrows indicate the condensation of chromatin; * indicates autophagosomes. Scale bars, 1 μ m. (E) Levels of apoptotic protein caspase 3 and antiapoptotic protein Bcl2 in podocytes by western blotting. (F) Western blots of Bax and cytochrome c in mitochondria and cytosol. Error bars represent mean \pm SEM. *P < 0.05 vs. Control; #P < 0.05 vs. PA. BBR, Berberine; PA, palmitate; SDs, slit diaphragm proteins; MMP-9, matrix metalloproteinase-9; TEM, transmission electron microscope.

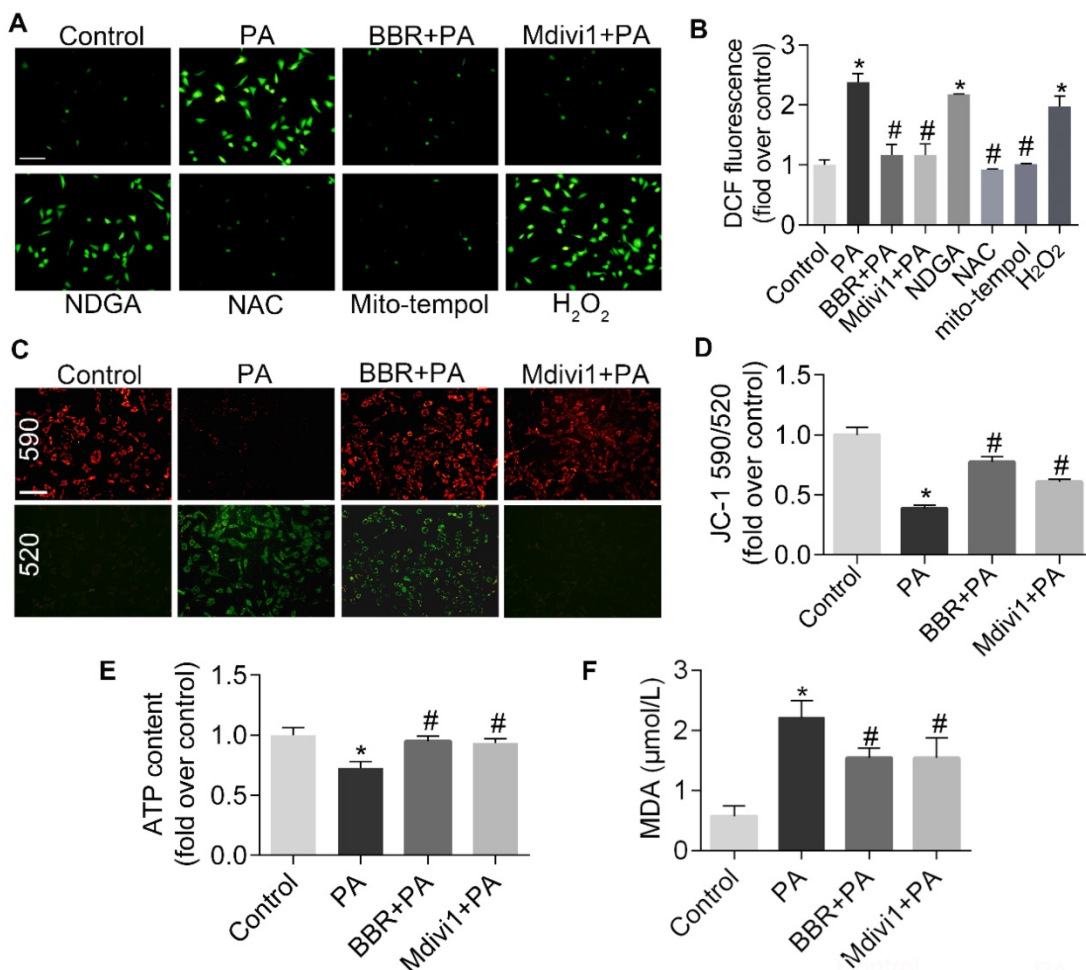


Figure 2. BBR inhibited PA-induced mtROS production and mitochondrial dysfunction in podocytes. (A, B) Cellular ROS production was detected by fluorescence microscopy (A) and flow cytometry (B) after DCFH-DA staining. Scale bar, 200 μm. (C, D) MMP was detected by fluorescence microscopy (C) and flow cytometry (D) after JC-1 staining. Scale bar, 200 μm. (E) ATP content were assayed in cells of different conditions. (F) MDA content was measured in podocytes. Error bars represent mean ± SEM. *P < 0.05 vs. Control; #P < 0.05 vs. PA. BBR, Berberine; PA, palmitate; ROS, mitochondrial reactive oxygen species; NDGA, nordihydroguaiaretic acid; NAC, N-acetylcysteine; DCF, dichlorofluorescein; MMP, mitochondrial membrane potential; ATP, adenosine triphosphate; MDA, malonaldehyde.

BBR blocks Drp1-mediated mitochondrial fission in podocytes cultured with PA

Since Drp1 is the critical mediator of mitochondrial fission, we next examined whether Drp1 activity in podocyte was influenced after PA and BBR intervention. As shown in Figure 4A-C, PA-induced overexpression of Drp1 in mRNA and protein were both abolished by BBR treatment. Besides, BBR could suppress Drp1 translocation to the mitochondria and suppress its phosphorylation at Serine 616 site. To further investigate the possible mechanism, we tested the expression of Drp1 receptors that may help recruit Drp1 to the MOM[48]. Our results showed that levels of mitochondrial fission protein (MFF), mitochondrial fission protein 1 (Fis1), mitochondrial dynamics proteins (Mid49, Mid51) were simultaneously down-regulated by BBR administration, but BBR failed to inhibit the gene transcription of these receptors (Figure 4D-E).

Given that oxidative stress can affect mitochondrial biogenesis and damage mtDNA[4], and BBR could significantly reverse mitochondria number decrease induced by PA as demonstrated above (Figure 3E), we thus evaluated several transcription factors that regulate mitochondrial biogenesis [49]. Peroxisome proliferator-activated receptor-γ co-activator 1α (PGC-1α) is the primary regulator of mitochondrial biogenesis and energy metabolic homeostasis[50]. We found that the expression levels of PGC-1α were upregulated by BBR (Figure 4E-F). Other markers of mitochondrial biogenesis were also checked and significantly increased in BBR group, including transcription factor A of mitochondria (TFAM), nuclear respiratory factors 1 and 2 (NRF1, NRF2). However, BBR failed to increase mtDNA copy number reflected by gene expression of ND1 (Figure 4F).

To further elucidate whether podocyte damage and mitochondria dysfunction could be induced by

directly increasing Drp1 level but prevented by Drp1 downregulation, we upregulated Drp1 expression by infecting podocytes with lentivirus expressing Drp1 and downregulated its level with Drp1-specific siRNA (with empty lentivirus and scramble oligonucleotide acting as controls, respectively). The role of Drp1 was confirmed in promoting cell injury and apoptosis (Figure 5A-E), mitochondrial dysfunction (Figure 6A-C), mitochondria fragmentation

(Figure 5D-E). The protective effects of BBR on PA-induced cell damage were largely abolished by Drp1 overexpression and enhanced by Drp1 downregulation (Figure 5A-E, Figure 6A-F). These results demonstrated that BBR might protect podocytes from PA-induced cell damage and mitochondrial dysfunction mainly through inhibiting mitochondria Drp1 activity.

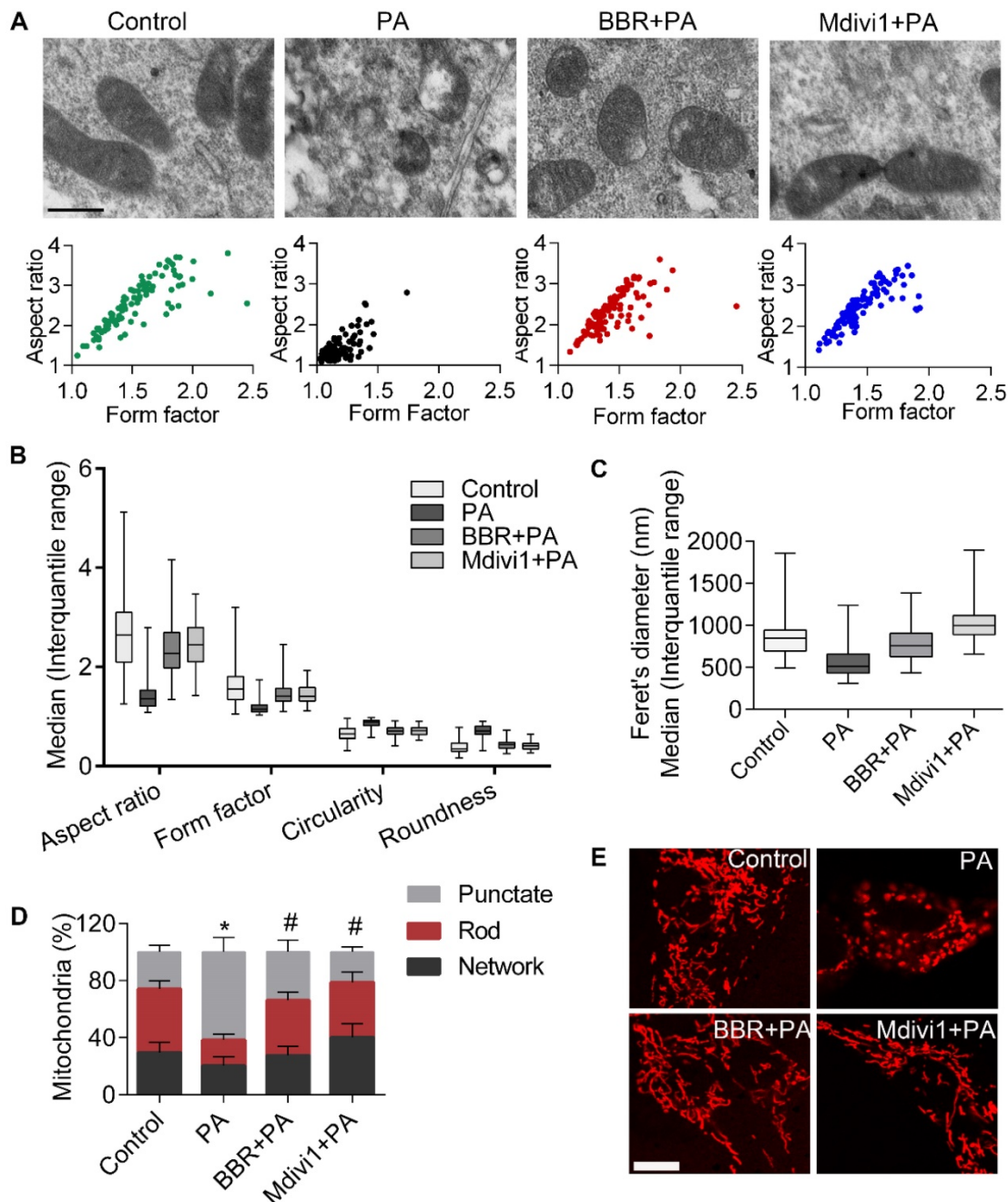


Figure 3. BBR inhibited PA-induced mitochondrial fragmentation in podocytes. (A) Mitochondrial morphology was observed by TEM and assessed by aspect ratio and form factor using Image J from three independent experiments (>100 mitochondria). Scale bars, 500 nm. (B) Aspect ratio, form factor, circularity, and roundness were quantified for each condition (>100 mitochondria). (C) Feret's diameter that reflects the longitudinal mitochondrial length was measured by Image J analysis (>100 mitochondria). (D) Quantification of the mitochondrial morphology shown in (E) by Image J analysis from three independent experiments (>500 mitochondria). (E) Mitochondria were stained by MitoTracker Red and imaged by laser scanning confocal microscopy. Scale bars, 10 μ m. Error bars represent mean \pm SEM, except morphological parameters of mitochondria shown as the median (interquartile range). * $P < 0.05$ vs. Control; # $P < 0.05$ vs. PA. BBR, Berberine; PA, palmitate; TEM, transmission electron microscope.

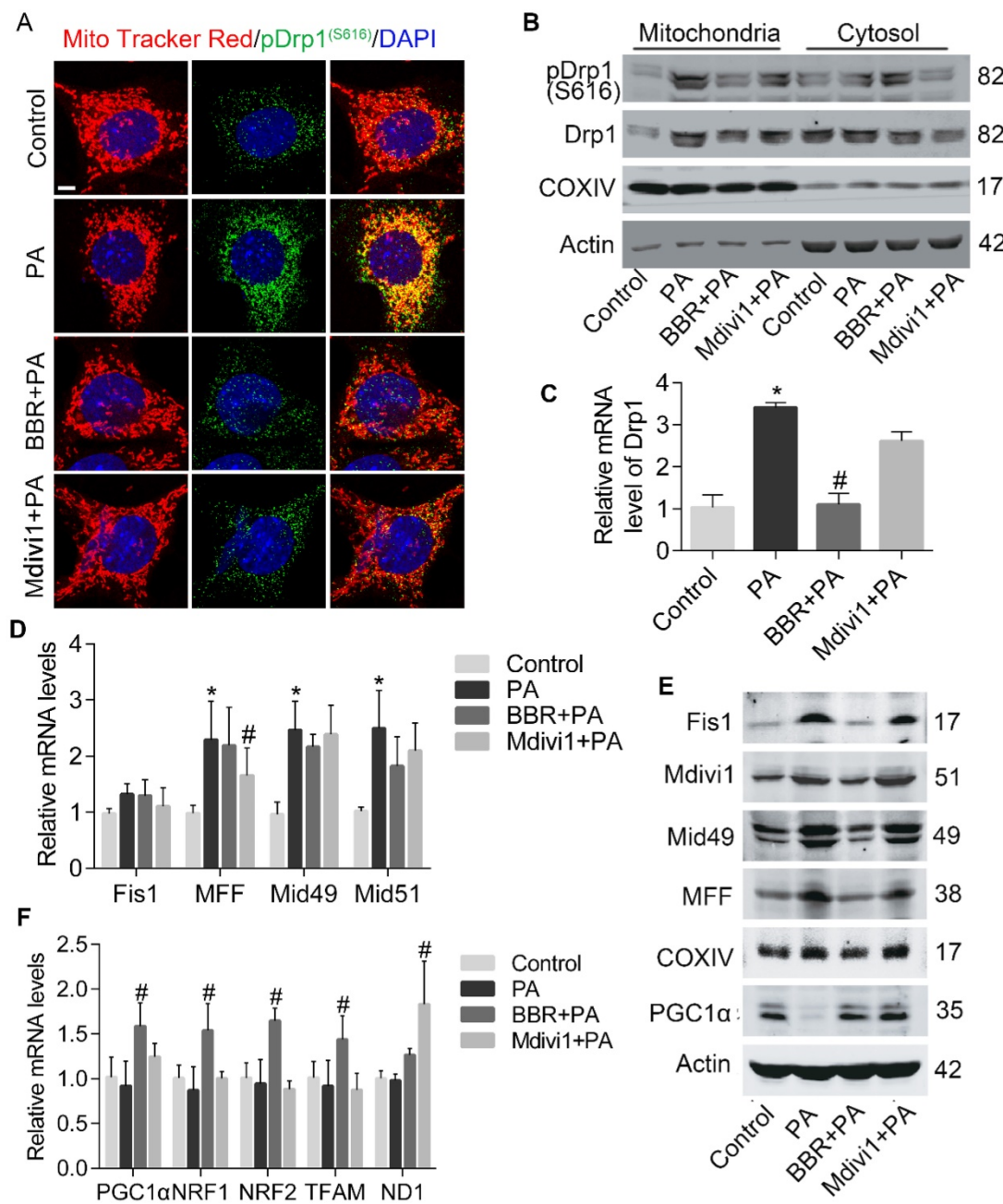


Figure 4. BBR prohibited PA-induced mitochondrial fission via regulating Drp1 in podocytes. (A) Immunofluorescence of MitoTracker and pDrp1 (S616). MitoTracker, red; pDrp1 (S616), green; DAPI, blue; merge, yellow. Scale bars, 10 μ m. (B) Western blotting of Drp1 and pDrp1 (S616) protein expression in mitochondria and cytosol. (C) Gene expression of Drp1 was determined by RT-PCR. (D) Mitochondrial fission-related gene expression profile in podocytes. (E) Western blots showing the levels of mitochondrial fission-related proteins. (F) Mitochondrial biogenesis-related gene expression in podocytes. Error bars represent mean \pm SEM. *P < 0.05 vs. Control; #P < 0.05 vs. PA. BBR, Berberine; PA, palmitate; Drp1, dynamin-related protein 1; RT-PCR, quantitative real-time PCR; Mid51 and Mid49, mitochondrial dynamics proteins of 51 and 49 kDa; Fis1, mitochondrial fission protein 1; MFF, mitochondrial fission protein; PGC1 α , peroxisome proliferator-activated receptor- γ co-activator 1 α ; TFAM, transcription factor A, mitochondrial; NRF1 and NRF2, nuclear respiratory factors 1 and 2.

BBR ameliorates DKD symptoms and protects glomerular podocytes in db/db mice

Then we evaluated whether BBR treatment in mouse models of DKD has analogous results found in cultured podocytes. As shown in Figure 7A-7E, body weight, FBG, plasma triglyceride (TG), microalbumin-to-creatinine ratios (ACR) and kidney FFA in db/db mice were all decreased with the treatment of BBR. And consistent with *in vitro* results that BBR could

prevent excessive FFA-induced podocyte injury, decreased expression of SDs and elevated protein level of desmin in glomerular podocytes from db/db mice were detected and reversed by BBR treatment (Figure 7F). We also observed that glomeruli from db/db mice exhibited decreased numbers of podocytes quantified by staining podocin (a podocyte-specific cytoplasmic protein) (Figure 7G, row 1), effacement of foot processes (Figure 7G, row

2), increased mesangial matrix accumulation (Figure 7H, row 1) and incrasation of glomerular basement membrane (Figure 7H, row 2). These pathological changes in diabetic mice were attenuated in different degrees with the treatment of BBR, similar to the histomorphology observed in nondiabetic controls. Through measuring the expression of

apoptotic family members, we found that podocyte apoptosis in db/db mice was significantly increased when compared with nondiabetic controls, and this was markedly improved with the administration of BBR (Figure 7I-J). Taken together, our data demonstrated the beneficial effect of BBR on the key symptoms of DKD.

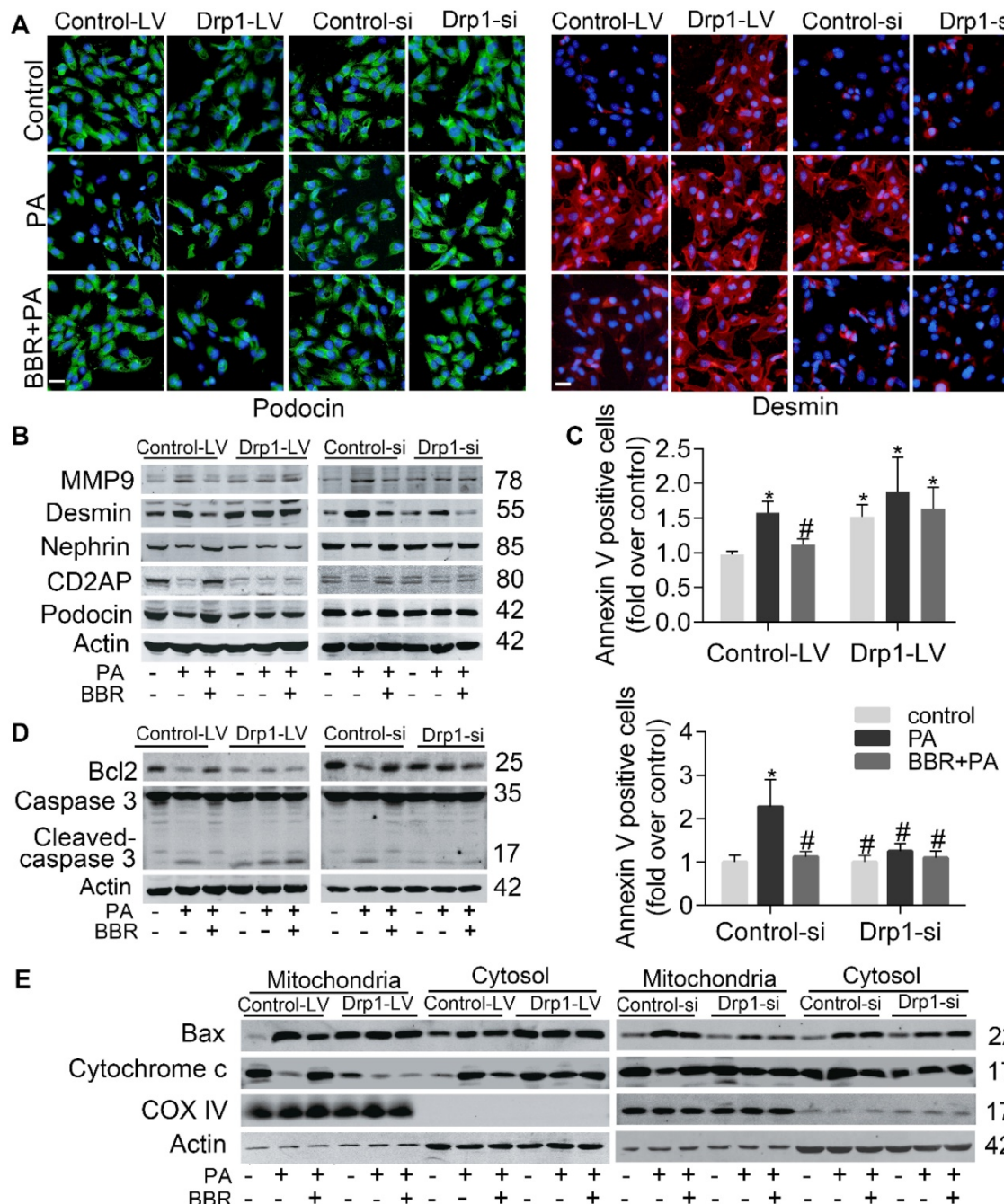


Figure 5. Upregulation and downregulation of Drp1 blunted and enhanced the effects of BBR on cell injury and apoptosis in PA-treated podocytes respectively. (A) Effects of Drp1 upregulation and downregulation on PA-induced podocyte injury in the presence or absence of BBR. Podocin (left panel) and desmin (right panel) protein expression were detected by fluorescence microscopy. Podocin, green; Desmin, red. Scale bars, 200 μ m. (B) Western blots indicating Drp1 upregulation (right panel) and downregulation (right panel) blunted and enhanced the effects of BBR on PA-induced podocyte injury respectively. (C) Effects of Drp1 upregulation (upper panel) and downregulation (lower panel) on PA-induced apoptosis in the presence or absence of BBR were measured by flow cytometry. (D) Effects of Drp1 upregulation (left panel) and downregulation (right panel) on podocyte apoptosis. Protein expression of apoptotic family members were detected by western blotting. (E) Cell apoptosis-associated Bax and cytochrome c levels in mitochondria and cytosol were assessed by western blotting after Drp1 upregulation (left panel) and downregulation (right panel). Error bars represent mean \pm SEM. *P < 0.05 vs. Control; #P < 0.05 vs. PA. BBR, Berberine; PA, palmitate; MMP-9, matrix metalloproteinase-9; Drp1, dynamin-related protein 1; LV, lentivirus; si, si RNA.

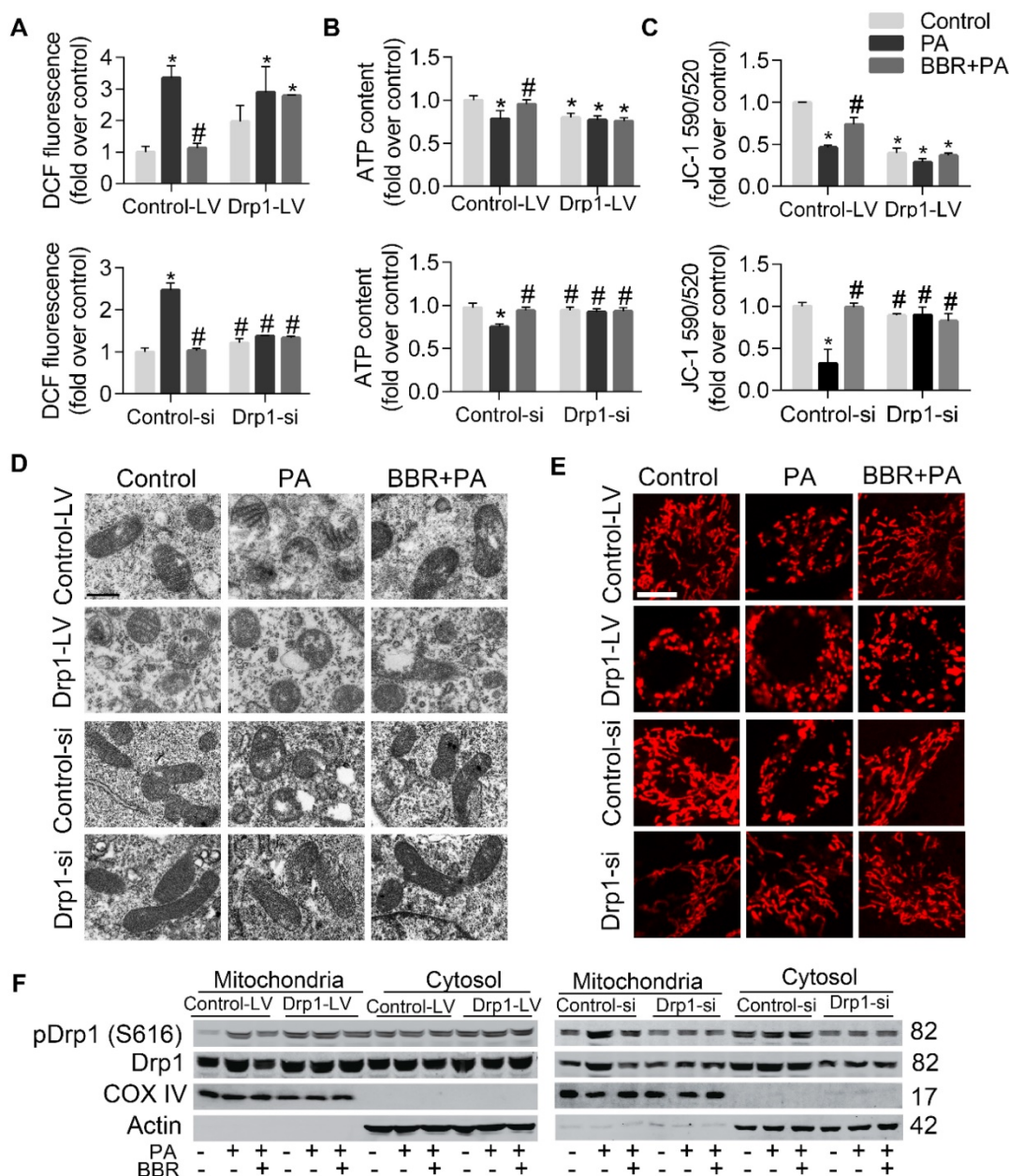


Figure 6. The effects of BBR on mitochondrial fission in PA-treated podocytes were blunted and enhanced by Drp1 upregulation and downregulation respectively. (A) Upregulation and downregulation of Drp1 blunted and enhanced the effects of BBR on cellular ROS production in PA-treated podocytes respectively, assessed by flow cytometry. (B) The effects of BBR on ATP production in PA-treated podocytes was blunted and enhanced by upregulation and downregulation of Drp1 respectively. (C) The effects of BBR on mitochondrial membrane potential in PA-treated podocytes were blunted and enhanced by upregulation and downregulation of Drp1 respectively, measured by flow cytometry. (D) The effects of BBR on mitochondrial morphology after upregulation and downregulation of Drp1 was observed by TEM. Scale bars, 500 nm. (E) The effects of BBR on mitochondrial morphology after upregulation and downregulation of Drp1 was visualized by MitoTracker Red. Scale bars, 10 μm. (F) Western blotting of Drp1 and pDrp1 (S616) protein expression in cytosol and mitochondria after upregulation and downregulation of Drp1. Error bars represent mean ± SEM. *P < 0.05 vs. Control; #P < 0.05 vs. PA. BBR, Berberine; PA, palmitate; Drp1, dynamin-related protein 1; ROS, reactive oxygen species; DCF, dichlorofluorescein; LV, lentivirus; si, si RNA; ATP, adenosine triphosphate; TEM, transmission electron microscope.

BBR prevents mitochondrial dysfunction of podocytes in DKD mice

We next tested the effect of BBR on podocyte mitochondria in DKD mice. Because increased FFA could induce excessive ROS which causes damage to mitochondria, we measured levels of oxidative stress in kidney tissue via DHE staining and found that these were markedly alleviated by BBR, both in

kidney glomeruli and tubules of diabetic mice (Figure 8A). Mitochondrial ultrastructure in diabetic glomerular podocytes showed punctate and round shape, whereas samples from BBR-treated mice had marked improvement in morphology with clearly elongated mitochondria (Figure 8B-C). Therefore, BBR treatment significantly prevented the mitochondrial fragmentation of podocytes in db/db mice.

Then we clarified the contribution of BBR in blocking Drp1-mediated mitochondrial fragmentation in DKD mice. The results showed that BBR markedly prevented Drp1 translocation to the mitochondria in podocytes from DKD (Figure 8D-E), as reflected by western blotting and immunofluorescence analysis. BBR also inhibited the gene transcription of Drp1 (Figure 8F). To further certify the role of BBR on mitochondrial fission, we detected Drp1 receptors (MFF, Fis1, Mid49 and Mid51) in DKD mice. Our data indicated that these protein levels were increased under DKD conditions and were reversed by BBR treatment (Figure 8G). Whereas the gene levels related

to mitochondria biogenesis did not show a significant decline in db/db mice, there exhibited a marked increase by BBR treatment (Figure 8H). Collectively, these results suggested that BBR could modulate mitochondrial dynamics through preventing Drp1 expression and translocation to the mitochondria and promoting mitochondria biogenesis.

Taken together, our findings revealed that Drp1 translocation from cytoplasm to mitochondria is a key event in the pathogenesis of DKD. The inhibition of Drp1 activity by BBR may be beneficial to enhancing mitochondrial fitness and slowing the progression of DKD.

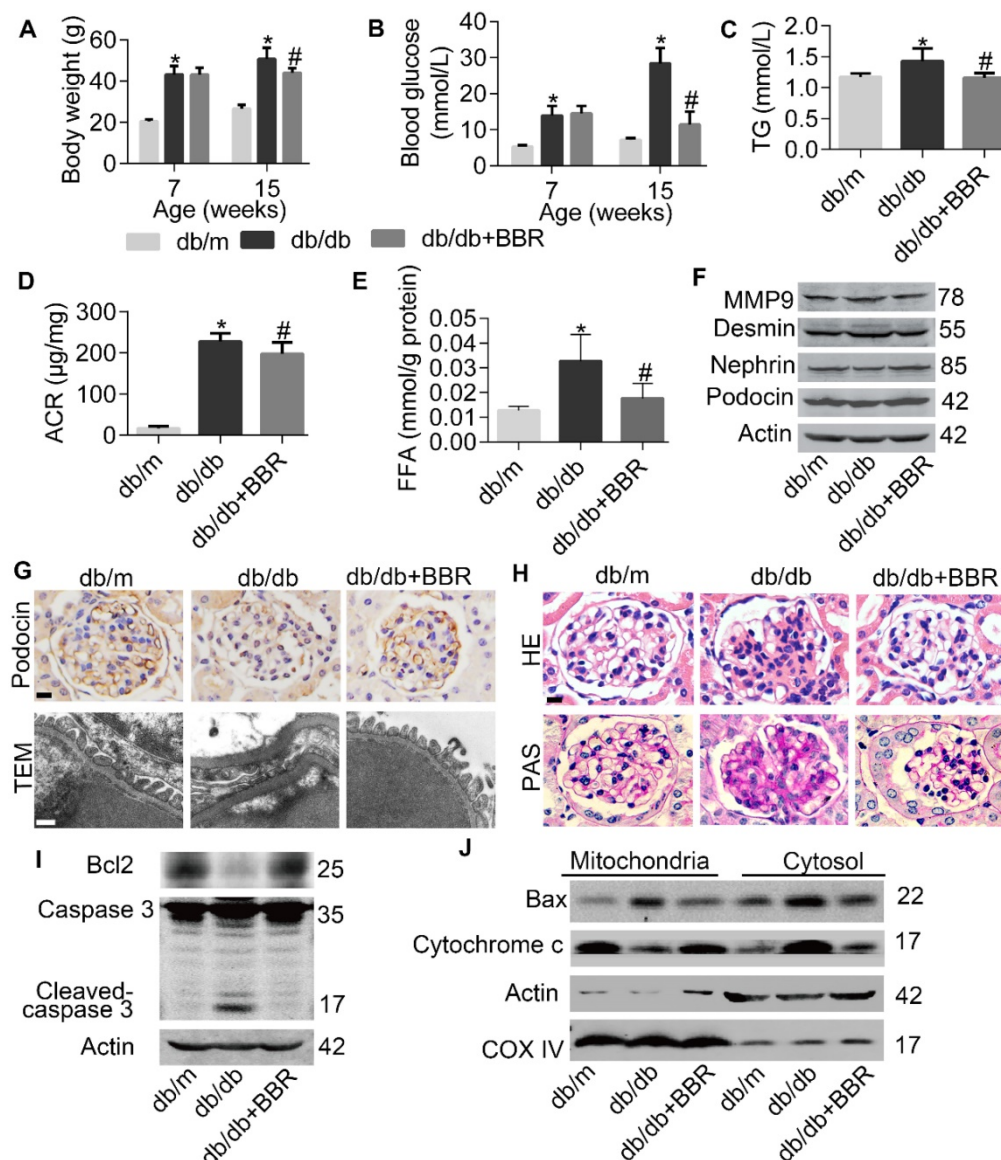


Figure 7. BBR prevented progression of DKD in db/db mice. (A) Body weight of mice before and after intervention. (B) Fasting blood glucose at two points. (C) Blood TG in different groups. (D) Microalbumin-to-creatinine ratios (ACR) in different groups. (E) FFA levels in kidney glomeruli from different groups. (F) SDS and markers of podocyte injury in kidney glomeruli were detected by western blotting. (G) Podocin staining of podocytes (row 1) and TEM of podocyte foot processes and glomerular basement membrane (row 2). Scale bars, 10 μm for row 1, 500 nm for row 2. (H) Representative micrographs of HE (row 1) and PAS (row 2)-stained kidney sections from different groups treated with or without BBR. Scale bars, 10 μm for row 1 and 2; (I) Levels of apoptotic family members in glomerular podocytes were detected by western blotting. (J) Western blotting reflected the levels of Mitochondrial and cytosolic Bax and cytochrome c in glomerular podocytes. Error bars represent mean ± SEM. *P < 0.05 vs. db/m; #P < 0.05 vs. db/db. BBR, berberine; TG, triglyceride; ACR, microalbumin-to-creatinine ratios; FFA, free fatty acids; DKD, diabetic kidney disease; HE, hematoxylin-eosin; PAS, periodic acid-schiff. SDS, slit diaphragm proteins; TEM, transmission electron micrographs.

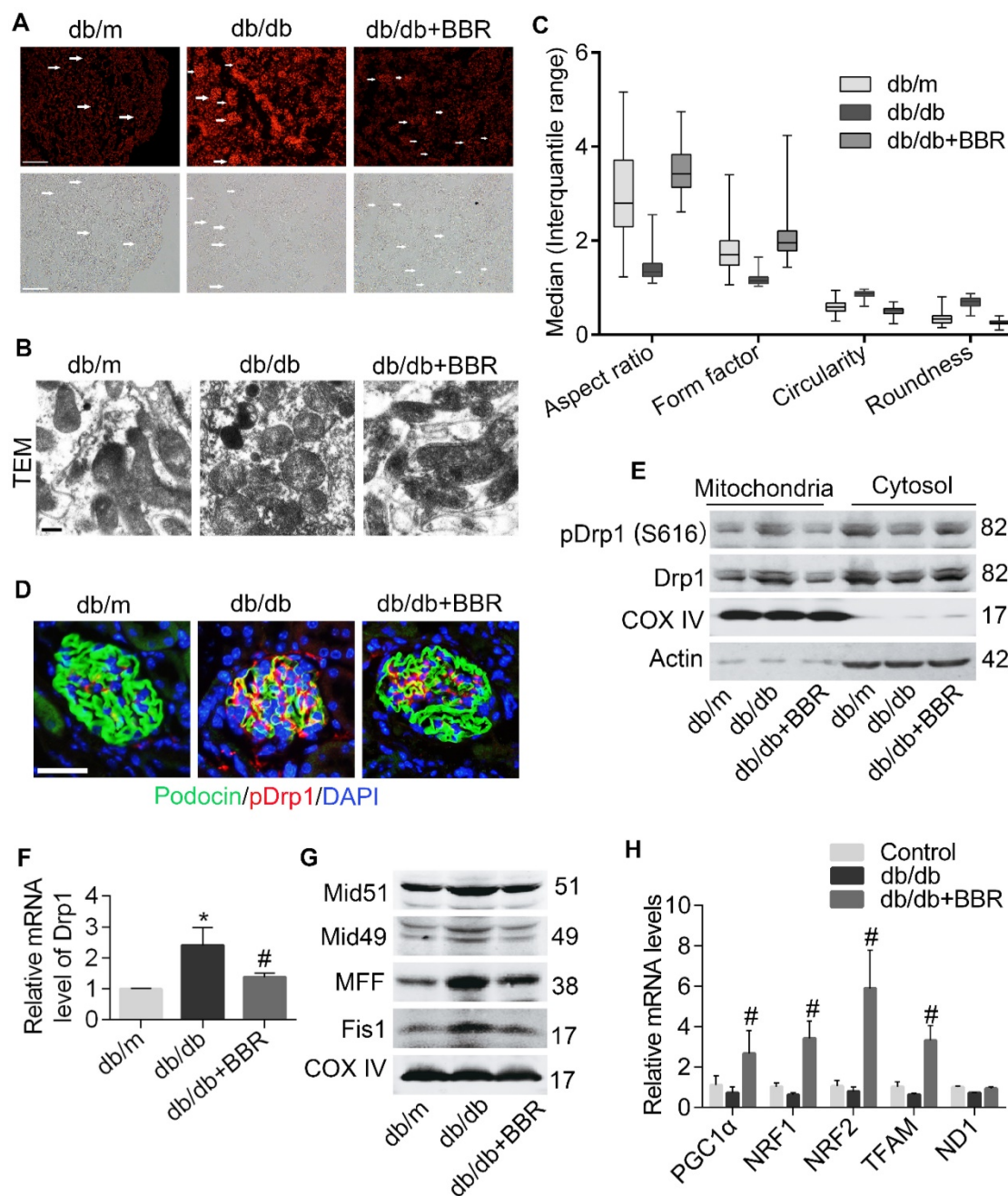


Figure 8. BBR attenuated Drp1-mediated mitochondrial fission in db/db mice. (A) The ROS content in glomeruli were measured by DHE staining. Arrows indicate the glomeruli. Scale bars, 200 μ m. (B, C) Mitochondrial morphology in glomerular podocytes was observed by TEM (B) and quantified by image j (C), as reflected by aspect ratio, form factor, circularity, and roundness. A minimum of 50 glomeruli in three sections per animal were assessed ($n = 5-8/\text{group}$, >100 mitochondria). Scale bars, 500 nm. (D) Immunofluorescence of kidney sections stained with podocin (green) and pDrp1 (S616) (red). Nuclei were counterstained with DAPI (blue). Scale bars, 50 μ m. (E) Western blotting of Drp1 and pDrp1 (S616) protein expression in glomerular podocytes. (F) Gene expression of Drp1 was determined in kidney glomeruli. (G) The changes of mitochondrial fission-related proteins in kidney glomeruli were assessed by western blotting. (H) Mitochondrial biogenesis-related gene expression in kidney glomeruli. Error bars represent mean \pm SEM, except morphological parameters of mitochondria shown as the median (interquartile range). * $P < 0.05$ vs. db/m; # $P < 0.05$ vs. db/db. BBR, berberine; ROS, reactive oxygen species; DHE, dihydroethidium; Drp1, dynamin-related protein 1; TEM, transmission electron micrograph; Mid51 and Mid49, mitochondrial dynamics proteins of 51 and 49 kDa; Fis1, mitochondrial fission protein 1; MFF, mitochondrial fission protein; PGC1 α , peroxisome proliferator-activated receptor- γ co-activator 1 α ; TFAM, transcription factor A, mitochondrial; NRF1 and NRF2, nuclear respiratory factors 1 and 2.

Discussion

In the current study, the renoprotective role of BBR associated with podocyte mitochondria and the underlying mechanism were explored. Our findings indicated that BBR could regulate the metabolic

abnormalities including hyperglycemia and dyslipidemia in db/db mice. BBR also ameliorated the symptoms of DKD by relieving glomerular sclerosis, albuminuria and podocyte damage *in vivo*. The possible mechanism is that BBR could alleviate FFA-induced podocyte injury through suppressing

Drp1-mediated mitochondrial dysfunction.

Previous studies suggested podocytes are highly sensitive to FFA. Enhanced FFA uptake by podocytes could lead to intracellular lipid accumulation and peroxidation, insulin resistance, endoplasmic reticulum stress and excessive ROS generation [22]. However, the specific molecular mechanism that couple FFA-induced ROS with podocytes apoptosis and the role of BBR remain unknown. Our results showed that elevated FFA could induce podocyte damage and excessive mtROS production, which could be abolished by BBR treatment via modulating Drp1-mediated mitochondrial dynamics. This was consistent with a recent research that podocyte-specific deletion of Drp1 in mouse model significantly reduced albuminuria and mitochondria fragmentation, accompanied by better mitochondrial fitness, increased oxygen consumption and ATP generation [9]. Another study found phosphorylating Drp1 at ser600 residue could promote its recruitment to the mitochondria, thus triggering hyperglycemia-induced mitochondrial fission in podocytes[51]. However, the two phosphorylation sites of Drp1 (ser616 and ser637) in mitochondrial fission have remained controversial [6, 7, 52]. Therefore, we examined both Drp1 ser616 and ser 637. Then we found only the protein levels of Drp1 ser616 were markedly different between groups both *in vivo* and *in vitro*. Our interpretation is that the effect of phosphorylation of Drp1 may be cell-type/tissue/stimulus dependent. Specifically, podocytes in our experimental models were pretreated with BBR/Mdivi1 before being exposed to PA. How the phosphorylation of Drp1 might regulate mitochondrial dynamics deserve further exploration in future research.

Recent Studies suggest excessive mitochondrial fission in human and mouse podocytes is closely linked to key features of DKD [10, 17]. Considering the pivotal role of mitochondrial dynamics disorder and ROS damage in the development of DKD, one study demonstrated that metformin, which is a well-known hypoglycemic drug, could markedly alleviate renal interstitial fibrosis and glomerular damage via regulation of oxidative stress-related gene expression[53]. Other research also found antioxidant agents could selectively accumulate in the mitochondrial matrix, thus reduce proteinuria and glomerular damage in diabetic mice[54-56]. For example, specific targeting of mitochondrial ROS with antioxidants could bring benefits to DKD rodent models by improving mitochondrial bioenergetics[57]. However, some limitations exist for current therapy targeting at mitochondrial oxidative metabolism. For example, since these are various cell biology, it can be very difficult to achieve the desired effect on cell type and

tissue specific without disturbing organs other than the kidney [58].

Our attempts to define the effects of BBR on mitochondria dysfunction indicated that BBR treatment could block Drp1-mediated mitochondrial damage and excessive ROS generation in podocytes. These results were consistent with previous findings that BBR could relieve endoplasmic reticulum stress and oxidative stress in aldosterone or high glucose-induced podocytes[27, 59]. The mechanism involved might be that BBR could ameliorate podocyte apoptosis and symptoms of DKD through regulating TLR4/NF- κ B pathway or TGF β 1/PI3K/AKT pathway[60-62]. Interestingly, researchers have recently demonstrated mitochondrial dysfunction in glomerular endothelial cells is the critical characteristic of DKD, which precedes podocyte apoptosis[57]. These findings not only provide new insights into how mitochondrial dysfunction in glomerular cells might exert great influence in the development of DKD, but also identified possible therapeutic targets for DKD treatments. BBR has also been tested to alleviate renal fibrosis via multiple signaling pathways, including regulation of NRF2 pathway, TGF- β /Smad pathway and Notch/snail pathway in renal tubular cells, and the AGEs-RAGE pathway in mesangial cells[63-66]. Further comprehensive investigation is needed to assess the multiple effects of BBR on renal cells in DKD, which could promote the clinical application of BBR and provide alternative therapy for DKD patients.

The investigation of renoprotective role of BBR was still limited to animal research. Although numerous clinical studies have demonstrated its strong effects in the treatment of DM[67-69], there was few studies at this stage about the usage of BBR in DKD patients. These previous results strongly suggested the efficacy and safety of BBR in treatment of patients with DM and dyslipidemia, with little side effects[38]. It is worth noting that functions of the liver and kidney were improved greatly with BBR treatment by regulating liver enzymes and improving renal function[38]. The mechanism of BBR in glucose-lowering action in target organs may be different, but there still exist similarities. Therefore, BBR might be a suitable substitute for DKD treatment in regulating metabolic abnormalities and relieving renal injury over long-term therapy, considering less cost and adverse effects. Large controlled clinical trials with high quality are needed to further assess the efficacy and safety of berberine in the treatment of DKD.

Previous discoveries have illuminated the novel correlation between mitochondrial fission and the progression of DKD and indicated Drp1 may be a potential therapeutic target in DKD. In the present

study, we found that through inhibiting the expression and translocation of Drp1, BBR potently improved the fragmentation and dysfunction of mitochondria in podocytes, reduced mesangial matrix expansion, GBM thickening, podocyte damage, albuminuria and metabolic abnormalities of DKD. In summary, our study provided the first evidence that inhibiting Drp1-mediated mitochondrial fission and cell apoptosis might be one of the possible mechanisms of BBR in preventing FFA-induced podocytes damage, which shed insights into the role of BBR as a new prospective agent against DKD. However, there still exist great challenges for future research in protecting podocytes for the treatment of DKD.

Abbreviations

FFA: free fatty acid; DKD: diabetic kidney disease; BBR: berberine; PA: palmitic acid; ROS: reactive oxygen species; Drp1: dynamin-related protein 1; mtDNA: mitochondrial DNA; ATP: adenosine triphosphate; MMP: mitochondrial membrane potential; MOM: mitochondrial outer membrane; GFB: glomerular filtration barrie; mtROS: mitochondrial ROS; DM: diabetes mellitus; SDs: slit diaphragm proteins; MMP-9: matrix metalloproteinase-9; TEM: transmission electron microscope; mtBax: mitochondria Bax; DCFH-DA: 2',7'-Dichlorofluorescein diacetate; NAC: antioxidant N-acetylcysteine; NDGA: nordihydroguaiaretic acid; MDA: malondialdehyde; MID51 and MID49: mitochondrial dynamics proteins of 51 and 49 kDa; FIS1: mitochondrial fission protein 1; MFF: mitochondrial fission protein; PGC1 α : peroxisome proliferator-activated receptor- γ co-activator 1 α ; TFAM: mitochondrial transcription factor A; NRF1 and NRF2: nuclear respiratory factors 1 and 2; ND1: NADH dehydrogenase subunit 1; GBM: glomerular basement membrane; DHE: dihydroethidium; HE: hematoxylin-eosin; PAS: periodic acid-schiff; FBG: fasting blood glucose; TG: triglyceride; ACR: microalbumin-to-creatinine ratios; NF- κ B: nuclear factor- κ B; TLR4: toll-like receptor 4; PI3K: phosphatidylinositol 3 kinase; AKT: protein kinase B; TGF β : transforming growth factor- β ; AGEs: advanced glycation end products; RAGE: receptor of advanced glycation end products.

Supplementary Material

Supplementary figures and tables.

<http://www.thno.org/v09p1698s1.pdf>

Acknowledgements

This study was supported by the National Natural Science Foundation of China (grant number 81473637, 81673928, 81874382, 81703869); the State Administration of Traditional Chinese Medicine

(grant number JDZX2015214).

Author contributions

Xin Qin conceived the experiments, contributed to research data and wrote the manuscript; Yan Zhao, Jing Gong, Wenyia Huang and Fen Yuan contributed to mouse experiments; Xin Qin and Hao Su contributed to cell experiments; Hui Dong and Fuer Lu reviewed the manuscript. Hui Dong, Fuer Lu, Ke Fang, Dingkun Wang, Jingbin Li, Lijun Xu and Xin Zou discussed the experiments and manuscript.

Competing Interests

The authors have declared that no competing interest exists.

References

1. Chan DC. Fusion and fission: interlinked processes critical for mitochondrial health. *Annu Rev Genet*. 2012; 46: 265-87.
2. Tilokani L, Nagashima S, Paupe V, et al. Mitochondrial dynamics: overview of molecular mechanisms. *Essays Biochem*. 2018; 62: 341-60.
3. Shirihai OS, Song M, Dorn GW, 2nd. How mitochondrial dynamism orchestrates mitophagy. *Circ Res*. 2015; 116: 1835-49.
4. Youle RJ, van der Blieck AM. Mitochondrial fission, fusion, and stress. *Science*. 2012; 337: 1062-5.
5. Smirnova E, Gripasic L, Shurland DL, et al. Dynamin-related protein Drp1 is required for mitochondrial division in mammalian cells. *Mol Biol Cell*. 2001; 12: 2245-56.
6. Hu C, Huang Y, Li L. Drp1-Dependent Mitochondrial Fission Plays Critical Roles in Physiological and Pathological Progresses in Mammals. *Int J Mol Sci*. 2017; 18: 18010144.
7. Michalska B, Duszynski J, Szymanski J. [Mechanism of mitochondrial fission - structure and function of Drp1 protein]. *Postepy Biochem*. 2016; 62: 127-37.
8. Estaquier J, Arnoult D. Inhibiting Drp1-mediated mitochondrial fission selectively prevents the release of cytochrome c during apoptosis. *Cell Death Differ*. 2007; 14: 1086-94.
9. Ayanga BA, Badal SS, Wang Y, et al. Dynamin-Related Protein 1 Deficiency Improves Mitochondrial Fitness and Protects against Progression of Diabetic Nephropathy. *J Am Soc Nephrol*. 2016; 27: 2733-47.
10. Galvan DL, Green NH, Danesh FR. The hallmarks of mitochondrial dysfunction in chronic kidney disease. *Kidney Int*. 2017; 92: 1051-7.
11. Nagata M. Podocyte injury and its consequences. *Kidney Int*. 2016; 89: 1221-30.
12. Lin JS, Susztak K. Podocytes: the Weakest Link in Diabetic Kidney Disease? *Curr Diab Rep*. 2016; 16: 45.
13. Bhargava P, Schnellmann RG. Mitochondrial energetics in the kidney. *Nat Rev Nephrol*. 2017; 13: 629-46.
14. Fakhruddin S, Alanazi W, Jackson KE. Diabetes-Induced Reactive Oxygen Species: Mechanism of Their Generation and Role in Renal Injury. *J Diabetes Res*. 2017; 2017: 8379327.
15. Susztak K, Raff AC, Schiffer M, et al. Glucose-induced reactive oxygen species cause apoptosis of podocytes and podocyte depletion at the onset of diabetic nephropathy. *Diabetes*. 2006; 55: 225-33.
16. Forbes JM, Coughlan MT, Cooper ME. Oxidative stress as a major culprit in kidney disease in diabetes. *Diabetes*. 2008; 57: 1446-54.
17. Lindblom R, Higgins G, Coughlan M, et al. Targeting Mitochondria and Reactive Oxygen Species-Driven Pathogenesis in Diabetic Nephropathy. *Rev Diabet Stud*. 2015; 12: 134-56.
18. Wu L, Parhofer KG. Diabetic dyslipidemia. *Metabolism*. 2014; 63: 1469-79.
19. Richieri GV, Kleinfeld AM. Unbound free fatty acid levels in human serum. *J Lipid Res*. 1995; 36: 229-40.
20. Van der Vusse GJ, Roemen TH. Gradient of fatty acids from blood plasma to skeletal muscle in dogs. *J Appl Physiol* (1985). 1995; 78: 1839-43.
21. Yuzefovich L, Wilson G, Rachek L. Different effects of oleate vs. palmitate on mitochondrial function, apoptosis, and insulin signaling in L6 skeletal muscle cells: role of oxidative stress. *Am J Physiol Endocrinol Metab*. 2010; 299: E1096-105.
22. Sieber J, Jehle AW. Free Fatty acids and their metabolism affect function and survival of podocytes. *Front Endocrinol (Lausanne)*. 2014; 5: 186.
23. Badal SS, Danesh FR. New insights into molecular mechanisms of diabetic kidney disease. *Am J Kidney Dis*. 2014; 63: S63-83.
24. Pang B, Zhao LH, Zhou Q, et al. Application of berberine on treating type 2 diabetes mellitus. *Int J Endocrinol*. 2015; 2015: 905749.
25. Wang Y, Tong Q, Shou JW, et al. Gut Microbiota-Mediated Personalized Treatment of Hyperlipidemia Using Berberine. *Theranostics*. 2017; 7: 2443-51.

26. Pirillo A, Catapano AL. Berberine, a plant alkaloid with lipid- and glucose-lowering properties: From in vitro evidence to clinical studies. *Atherosclerosis*. 2015; 243: 449-61.
27. Wang B, Xu X, He X, et al. Berberine Improved Aldo-Induced Podocyte Injury via Inhibiting Oxidative Stress and Endoplasmic Reticulum Stress Pathways both In Vivo and In Vitro. *Cell Physiol Biochem*. 2016; 39: 217-28.
28. Mundel P, Heid HW, Mundel TM, et al. Synaptopodin: an actin-associated protein in telencephalic dendrites and renal podocytes. *J Cell Biol*. 1997; 139: 193-204.
29. Jentzsch AM, Bachmann H, Furst P, et al. Improved analysis of malondialdehyde in human body fluids. *Free Radic Biol Med*. 1996; 20: 251-6.
30. Luo JD, Wang YY, Fu WL, et al. Gene therapy of endothelial nitric oxide synthase and manganese superoxide dismutase restores delayed wound healing in type 1 diabetic mice. *Circulation*. 2004; 110: 2484-93.
31. Park KS, Wiederkehr A, Kirkpatrick C, et al. Selective actions of mitochondrial fission/fusion genes on metabolism-secretion coupling in insulin-releasing cells. *J Biol Chem*. 2008; 283: 33347-56.
32. Toyama EQ, Herzog S, Courchet J, et al. Metabolism. AMP-activated protein kinase mediates mitochondrial fission in response to energy stress. *Science*. 2016; 351: 275-81.
33. Valente AJ, Maddalena LA, Robb EL, et al. A simple ImageJ macro tool for analyzing mitochondrial network morphology in mammalian cell culture. *Acta Histochem*. 2017; 119: 315-26.
34. Picard M, White K, Turnbull DM. Mitochondrial morphology, topology, and membrane interactions in skeletal muscle: a quantitative three-dimensional electron microscopy study. *J Appl Physiol* (1985). 2013; 114: 161-71.
35. He L, Chinnery PF, Durham SE, et al. Detection and quantification of mitochondrial DNA deletions in individual cells by real-time PCR. *Nucleic Acids Res*. 2002; 30: e68.
36. Dong Y, Chen YT, Yang YX, et al. Metabolomics Study of Type 2 Diabetes Mellitus and the AntiDiabetic Effect of Berberine in Zucker Diabetic Fatty Rats Using Uplc-ESI-Hdms. *Phytother Res*. 2016; 30: 823-8.
37. Zhou J, Zhou S. Berberine regulates peroxisome proliferator-activated receptors and positive transcription elongation factor b expression in diabetic adipocytes. *Eur J Pharmacol*. 2010; 649: 390-7.
38. Lan J, Zhao Y, Dong F, et al. Meta-analysis of the effect and safety of berberine in the treatment of type 2 diabetes mellitus, hyperlipemia and hypertension. *J Ethnopharmacol*. 2015; 161: 69-81.
39. Katsuya K, Yaoita E, Yoshida Y, et al. An improved method for primary culture of rat podocytes. *Kidney Int*. 2006; 69: 2101-6.
40. Liu L, Fu W, Xu J, et al. Effect of BMP7 on podocyte transdifferentiation and Smad7 expression induced by hyperglycemia. *Clin Nephrol*. 2015; 84: 95-9.
41. Li SY, Huang PH, Yang AH, et al. Matrix metalloproteinase-9 deficiency attenuates diabetic nephropathy by modulation of podocyte functions and dedifferentiation. *Kidney Int*. 2014; 86: 358-69.
42. Prokhorova EA, Zamaraev AV, Kopeina GS, et al. Role of the nucleus in apoptosis: signaling and execution. *Cell Mol Life Sci*. 2015; 72: 4593-612.
43. Jin Y, Liu S, Ma Q, et al. Berberine enhances the AMPK activation and autophagy and mitigates high glucose-induced apoptosis of mouse podocytes. *Eur J Pharmacol*. 2017; 794: 106-14.
44. Rushworth GF, Megson IL. Existing and potential therapeutic uses for N-acetylcysteine: the need for conversion to intracellular glutathione for antioxidant benefits. *Pharmacol Ther*. 2014; 141: 150-9.
45. Yang SG, Park HJ, Kim JW, et al. Mito-TEMPO improves development competence by reducing superoxide in preimplantation porcine embryos. *Sci Rep*. 2018; 8: 10130.
46. Artega S, Andrade-Cetto A, Cardenas R. Larrea tridentata (Creosote bush), an abundant plant of Mexican and US-American deserts and its metabolite nordihydroguaiaretic acid. *J Ethnopharmacol*. 2005; 98: 231-9.
47. Kong Y, Trabucco SE, Zhang H. Oxidative stress, mitochondrial dysfunction and the mitochondria theory of aging. *Interdiscip Top Gerontol*. 2014; 39: 86-107.
48. Loson OC, Song Z, Chen H, et al. Fis1, Mff, MiD49, and MiD51 mediate Drp1 recruitment in mitochondrial fission. *Mol Biol Cell*. 2013; 24: 659-67.
49. Gleyzer N, Vercauteren K, Scarpulla RC. Control of mitochondrial transcription specificity factors (TFB1M and TFB2M) by nuclear respiratory factors (NRF-1 and NRF-2) and PGC-1 family coactivators. *Mol Cell Biol*. 2005; 25: 1354-66.
50. Villena JA. New insights into PGC-1 coactivators: redefining their role in the regulation of mitochondrial function and beyond. *Febs J*. 2015; 282: 647-72.
51. Wang W, Wang Y, Long J, et al. Mitochondrial fission triggered by hyperglycemia is mediated by ROCK1 activation in podocytes and endothelial cells. *Cell Metab*. 2012; 15: 186-200.
52. Chang CR, Blackstone C. Dynamic regulation of mitochondrial fission through modification of the dynamin-related protein Drp1. *Ann N Y Acad Sci*. 2010; 1201: 34-9.
53. Alhaider AA, Korashy HM, Sayed-Ahmed MM, et al. Metformin attenuates streptozotocin-induced diabetic nephropathy in rats through modulation of oxidative stress genes expression. *Chem Biol Interact*. 2011; 192: 233-42.
54. Pedraza-Chaverri J, Sanchez-Lozada LG, Osorio-Alonso H, et al. New Pathogenic Concepts and Therapeutic Approaches to Oxidative Stress in Chronic Kidney Disease. *Oxid Med Cell Longev*. 2016; 2016: 6043601.
55. Chacko BK, Reily C, Srivastava A, et al. Prevention of diabetic nephropathy in *Ins2(+/-)(-)(Akita)* mice by the mitochondria-targeted therapy MitoQ. *Biochem J*. 2010; 432: 9-19.
56. Hou Y, Li S, Wu M, et al. Mitochondria-targeted peptide SS-31 attenuates renal injury via an antioxidant effect in diabetic nephropathy. *Am J Physiol Renal Physiol*. 2016; 310: F547-59.
57. Qi H, Casalena G, Shi S, et al. Glomerular Endothelial Mitochondrial Dysfunction Is Essential and Characteristic of Diabetic Kidney Disease Susceptibility. *Diabetes*. 2017; 66: 763-78.
58. Yang S, Han Y, Liu J, et al. Mitochondria: A Novel Therapeutic Target in Diabetic Nephropathy. *Curr Med Chem*. 2017; 24: 3185-202.
59. Ni WJ, Ding HH, Tang LQ. Berberine as a promising anti-diabetic nephropathy drug: An analysis of its effects and mechanisms. *Eur J Pharmacol*. 2015; 760: 103-12.
60. Zhu L, Han J, Yuan R, et al. Berberine ameliorates diabetic nephropathy by inhibiting TLR4/NF-kappaB pathway. *Biol Res*. 2018; 51: 9.
61. Wang YY, Tang LQ, Wei W. Berberine attenuates podocytes injury caused by exosomes derived from high glucose-induced mesangial cells through TGFBeta1-PI3K/AKT pathway. *Eur J Pharmacol*. 2018; 824: 185-92.
62. Wu F, Yao DS, Lan TY, et al. Berberine prevents the apoptosis of mouse podocytes induced by TRAF5 overexpression by suppressing NF-kappaB activation. *Int J Mol Med*. 2018; 41: 555-63.
63. Li Z, Zhang W. Protective effect of berberine on renal fibrosis caused by diabetic nephropathy. *Mol Med Rep*. 2017; 16: 1055-62.
64. Qiu YY, Tang LQ, Wei W. Berberine exerts renoprotective effects by regulating the AGEs-RAGE signaling pathway in mesangial cells during diabetic nephropathy. *Mol Cell Endocrinol*. 2017; 443: 89-105.
65. Zhang X, He H, Liang D, et al. Protective Effects of Berberine on Renal Injury in Streptozotocin (STZ)-Induced Diabetic Mice. *Int J Mol Sci*. 2016; 17: 1327.
66. Yang G, Zhao Z, Zhang X, et al. Effect of berberine on the renal tubular epithelial-to-mesenchymal transition by inhibition of the Notch/snail pathway in diabetic nephropathy model KKAY mice. *Drug Des Devel Ther*. 2017; 11: 1065-79.
67. Zhang Y, Li X, Zou D, et al. Treatment of type 2 diabetes and dyslipidemia with the natural plant alkaloid berberine. *J Clin Endocrinol Metab*. 2008; 93: 2559-65.
68. Zhang H, Wei J, Xue R, et al. Berberine lowers blood glucose in type 2 diabetes mellitus patients through increasing insulin receptor expression. *Metabolism*. 2010; 59: 285-92.
69. Gu Y, Zhang Y, Shi X, et al. Effect of traditional Chinese medicine berberine on type 2 diabetes based on comprehensive metabolomics. *Talanta*. 2010; 81: 766-72.